Polymer 50 (2009) 5765–5770

Contents lists available at ScienceDirect

Polymer

journal homepage: www.elsevier.com/locate/polymer

Hydration mechanism on a poly(methacrylic acid) film studied by *in situ* attenuated total reflection infrared spectroscopy

Tomokazu Tajiri [a,b], Shigeaki Morita [c], Yukihiro Ozaki [a,*]

[a] Department of Chemistry, School of Science and Technology, Kwansei-Gakuin University, Sanda, Hyogo 669-1337, Japan
[b] Pharmaceutical Analysis, Pharmaceutical Research & Technology Laboratories, Technology, Astellas Pharma Inc., Yaizu, Shizuoka 425-0072, Japan
[c] EcoTopia Science Institute, Nagoya University, Nagoya, Aichi 464-8603, Japan

ARTICLE INFO

Article history:
Received 24 March 2009
Received in revised form
5 September 2009
Accepted 19 September 2009
Available online 8 October 2009

Keywords:
Poly(methacrylic acid) (PMAA)
Hydrogen bonding
Hydration

ABSTRACT

A drastic structure change during a hydration process of a poly(methacrylic acid) (PMAA) film was observed by time-resolved *in situ* attenuated total reflection infrared (ATR-IR) spectroscopy. Inter- or intra-hydrogen-bonds via side-chain carboxyl groups are formed as cyclic dimers, side-on dimers and linear open chain oligomers including open dimers in a dried PMAA film. By contacting water, the side-chain hydrogen-bonds in PMAA are dissociated instantly, and then the subsequent carboxyl groups which have no hydrogen-bond newly hydrate with water molecules in a side-on form. Quantum chemical calculations (QCCs) using a model monomer of propionic acid (PA) also support the hydrogen-bonded and hydrated structures explored by the ATR-IR spectroscopy. It has been concluded from the present study that the dissociation of hydrogen-bonded and newly created hydrated structures via the carboxyl groups play an important role for the swelling of PMAA in water.

1. Introduction

Poly(methacrylic acid) (PMAA) and its derivatives have widely been applied to pharmaceutical products as a pH-responsive enteric coating agent, a kind of drug delivery systems (DDS), to control the drug releasing in oral administration [1–3]. The quality of their drugs have been usually evaluated about only active ingredients by *in vivo* as a blood drug concentration in clinical practice or *in vitro* as a drug dissolution ratio from their products following the dissolution tests described in each Pharmacopoeia [4–6]. However, in order to clarify the drug releasing mechanisms of DDS products, the investigation of inherent physical properties and dissolution mechanisms of pharmaceutical functional excipients in water are of great importance.

There has been a number of studies on dried and hydrated structures of various kinds of polymers and the states of water interacting with the polymers [7–11], and the structures of water soluble polymer solutions have also been studied [12]. However, little attention has been paid to the hydration and dissolving process of hydrophilic polymers, because it is difficult to monitor their flash structure changes in water. To overcome the difficulty we have recently applied high-speed scan attenuated total reflection infrared (ATR-IR) spectroscopy equipped with a flow through cell (Fig. 1). The flow through cell method allows us to measure a process of water sorption into a polymer film [7].

Hydrogen-bonded and hydrated structures of carboxylic acids such as formic acid, acetic acid and propionic acid (PA) have well been studied by Raman spectroscopy [13–17], IR spectroscopy [14,18,19], X-ray diffraction [20] and nuclear magnetic resonance (NMR) [21]. Furthermore, several quantum chemical calculations (QCCs) have also been applied for such studies [21–28]. It has been reported that carboxylic acid groups form several associated conformations via hydrogen-bonds, namely cyclic dimers, side-on dimers and linear open chain oligomers including open dimers [29,30], and it is well-known that cyclic dimers dominate in the pure liquid or solid states of carboxylic acids [12–20].

Hydrated structures of carboxylic acid monomers have also been studied by using various techniques and QCCs [28,31–33]. In the field of polymers, there has been a great attention on the structures and their changes of hydrogen-bonded and hydrated poorly water soluble polymers [34], however, many of previous studies on carboxylic acid groups in polymers have dealt almost exclusively with the structures in solid forms and those in aqueous solutions, separately.

In this study, the hydration process of carboxyl groups in a water soluble hydrophilic PMAA film is explored by using rapid-scan ATR-IR spectroscopy with a flow through cell, because it allows us to evaluate simultaneously both the structures of hydrogen-bonded PMAA in

* Corresponding author. Tel.:+81 79 565 8349; fax: +81 79 565 9077.
E-mail address: ozaki@kwansei.ac.jp (Y. Ozaki).

0032-3861/$ – see front matter © 2009 Elsevier Ltd. All rights reserved.
doi:10.1016/j.polymer.2009.09.060

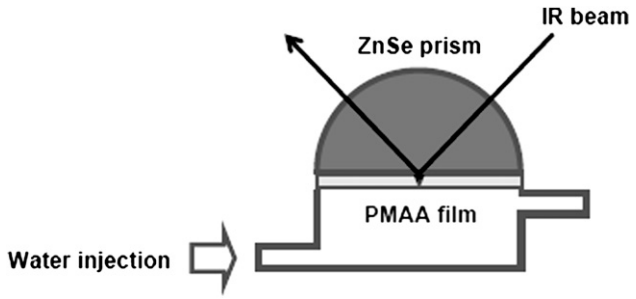

Fig. 1. Schematic illustration of the *in situ* ATR-IR flow-through cell used.

a solid state and those of hydrated one in a gel and a liquid under the same conditions, and furthermore, to detect time-resolved structural changes. Additionally, obtained spectra-structure correlations are examined by QCCs based on density functional theory (DFT) using a model monomer of PA instead of a real polymer of PMAA.

2. Experimental

2.1. Materials

An atactic PMAA was purchased from Polysciences, Inc. (averaged molecular weight of ca. 1.0×10^5). Methanol labeled guaranteed grade was purchased from Kanto Chemical. Water with a resistivity of 18.2 MΩ cm was prepared by use of a Milli-Q system.

A PMAA film was deposited on a hemispherical Zinc–Selenium (ZnSe) prism by 150 μL solvent-casting method of 10 mg/mL methanol solution and was dried at 80 °C for 3 h. A PMAA aqueous solution was prepared by stirring excessive amounts of PMAA in water over night at room temperature.

2.2. IR measurements

All the ATR-IR spectra were measured at a resolution of 4 cm^{-1} by using a Thermo Electron Nexus 470 Fourier-transform IR spectrometer equipped with a Seagull variable angle reflection accessory and a liquid nitrogen cooled HgCdTe detector. A prism with an adhered polymer film was mounted onto a homemade flow-through cell shown in Fig. 1. More detailed information about the cell was described elsewhere [7]. IR beam was introduced into the prism at an incident angle of 45°, which is larger than the critical angle of ca. 34°. A total of 64 scans were co-added to obtain each spectrum. ATR-IR spectra of liquid samples were measured using the same flow-through cell at the prism/liquid interface without a polymer film. Hydration process of a PMAA film was investigated by pouring water into the flow-through cell. In order to achieve such high-speed scans, a velocity of the moving mirror in the interferometer of 6.33 cm s^{-1} (100 kHz) was applied. A total of 2 scans, every 0.20 s from 0 to 30 s, were co-added to obtain each spectrum and a total of 148 spectra were measured. All the ATR-IR spectra were defined in an absorbance unit as

$$A = -\log_{10}\frac{R}{R_0} \tag{1}$$

where R and R_0 are intensities of the ATR-IR light from a sample and a reference, respectively. All the ATR-IR spectra were not subjected to Kramers–Kronig transformation and ATR correction. Note that a penetration depth of the evanescent wave can be estimated as

$$d_p = \frac{\lambda/n_{\mathrm{prism}}}{2\pi\sqrt{\sin^2\theta - \left(n_{\mathrm{sample}}/n_{\mathrm{prism}}\right)^2}} \tag{2}$$

where λ, n and θ are a wavelength of the near-field light, a refractive index and an incident angle into the prism, respectively [35]. Since the thickness of the film sample of ca. 3 μm is enough thicker than the penetration depth of ca. 0.9 μm at 1700 cm^{-1}, ATR-IR absorption by bulk water contacting with polymer film surface is never detected. The second derivative spectra were calculated by the Savitzky–Golay method [36] using homemade software after the spectra were subjected to Kawata–Minami smoothing [37]. In the present study, the curve-fitting spectra were obtained with software named SPINA 3.0 (Y. Katsumoto, Kwansei Gakuin University).

2.3. Quantum chemical calculations

All QCCs were performed based on DFT using a B3LYP function and a 6–31G(d) base set. The calculations of optimized structures, vibrational frequencies, IR intensities and self-consistent fields (SCF) were carried out with the Gaussian 03 program [38–40]. The force fields calculated at the B3LYP/6–31G(d) level were scaled down using a single scale factor of 0.9613, which is accepted to be the best for the level [41]. In order to estimate hydrogen-bonded and hydrated structures of PMAA, a model monomer of PA was used for the QCCs.

All the calculated spectra were constructed assuming a Lorentzian band shape with a 7 cm^{-1} band width. In addition, DFT calculations on the basis of the Onsager reaction field model [42,43] were performed to investigate the effects of hydration of PA on the IR spectra as a simple model of PMAA.

The energy of intermolecular interaction due to hydrogen-bond and hydration is defined as a energy difference before and after separation of each optimized hydrogen-bonded and hydrated structures, respectively. It was calculated using their SCF energies.

2.4. Gravimetric measurement

A PMAA film was prepared on a cover-glass for microscope by the same method as that of the ATR-IR measurement. After drying, water was cast and held on the PMAA dry film for around 30 s. After wiping the superfluous liquid water on the surface of the film, the weight of sample was measured before and after liquid water evaporating.

3. Results and discussion

3.1. ATR-IR spectra

Fig. 2a shows an ATR-IR spectrum in the 4000–1000 cm^{-1} region of a PMAA film dried by nitrogen gas flow in the cell. A broad feature overlapping with several weak peaks is observed in the 3700–2300 cm^{-1} region. Relatively sharp peaks in the 3000–2700 cm^{-1} region are assigned to C–H stretching modes of PMAA. O–H stretching bands are observed in the 3700–3000 cm^{-1} region [7–11]. A lower wavenumber bands in the 2700–2300 cm^{-1} region is assigned to overtones and combination of bands near 1391 and 1262 cm^{-1} enhanced by Fermi resonance with the broad O–H stretching band [29]. The most intensive bands in the 1750–1680 cm^{-1} region are identified as C=O stretching bands. The assignments for major IR bands in the 4000–1000 cm^{-1} region are summarized in Table 1. Fig. 3 shows a close-up spectrum and curve fitting spectra in the C=O stretching region of the dried PMAA film shown in Fig. 2a. Overlapped C=O peaks are deconvoluted by four curve fitting components corresponding to the non-hydrogen-bonded monoers, cyclic dimers, side-on dimers and linear oligomers of side-chain carboxyl groups in PMAA based on the second derivative result and the previously reported [29]. The four peaks observed and estimated at 1736, 1719, 1695 and 1679 cm^{-1} are

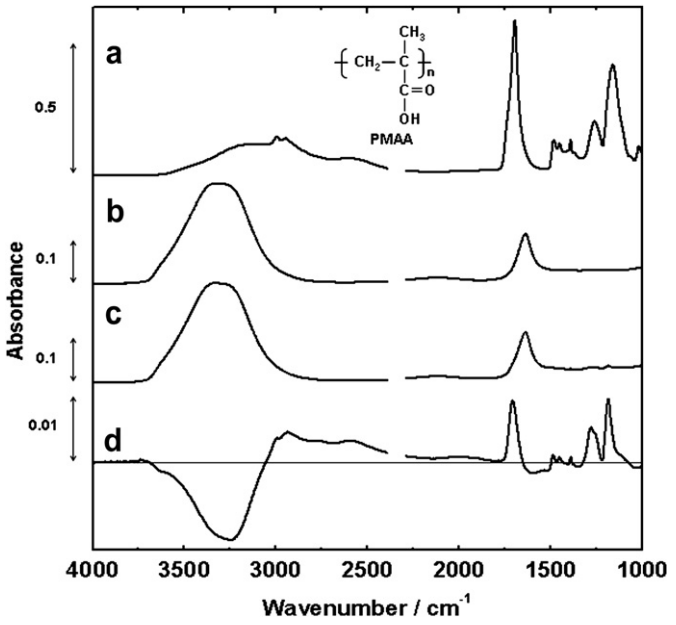

Fig. 2. ATR-IR spectra in the 4000–1000 cm^{-1} region of (a) a dried PMAA film, (b) bulk water and (c) a 57.6 mg mL^{-1} PMAA aqueous solution. (d) Difference spectrum obtained by the subtraction of water spectrum from the spectrum of the PMAA aqueous solution; (c)-(b).

assigned to C═O stretching bands of monomer (non-hydrogen bonded), side-on and cyclic dimeric hydrogen bonded, and linear oligomeric hydrogen bonded, respectively (Table 2). The assignments are also confirmed by QCCs for PA, the model compound of PMAA (Table 2).

Fig. 2b shows an ATR-IR spectrum in the 4000–1000 cm^{-1} region of bulk water measured from a ZnSe/water interface directly. An intense and broad O–H stretching band in the 3700–3000 cm^{-1} region and an O–H deformation band in the 1750–1550 cm^{-1} region are identified in the ATR-IR spectrum of water.

Fig. 2c and d shows an ATR-IR spectrum of a 57.6 mg mL^{-1} PMAA aqueous solution and a difference spectrum calculated by the subtraction of the spectrum of water from that of the PMAA aqueous solution, respectively. The spectrum of the PMAA aqueous solution is very close to that of bulk water in the whole spectral region except for a few small peaks observed in the finger print region. The assignments for major IR bands in the spectrum of Fig. 2d are also listed in Table 1. In the aqueous solution, most of the carboxylic acid groups of PMAA are not dissociated, because an asymmetric stretching COO^- band is not detected at around 1550 cm^{-1} [30].

Table 1
Band assignments of IR spectra of a dried PMAA film and an aqueous PMAA solution.

Frequency [ν/cm^{-1}]		Assignments
Dry film	Aqueous solution	
3205 broad	3552	O–H stretching
2995	2997	CH_3 asymmetric stretching
2942	2942	CH_2 antisymmetric stretching
2610	2585	Overtone and combination of bands near 1391 and 1262 cm^{-1} enhanced by Fermi resonance with the broad O–H stretching band
1693	1708	C═O stretching
1483	1486	CH_3 asymmetric bending
1447	1447	CH_2 scissoring
1391	1389	CH_3 symmetric bending
1262	1285	C–C–O stretching
1242	1256	C–C–O stretching
1185	1185	C–O stretching coupled with O–H in-plane bending
1154	1138	C–O stretching

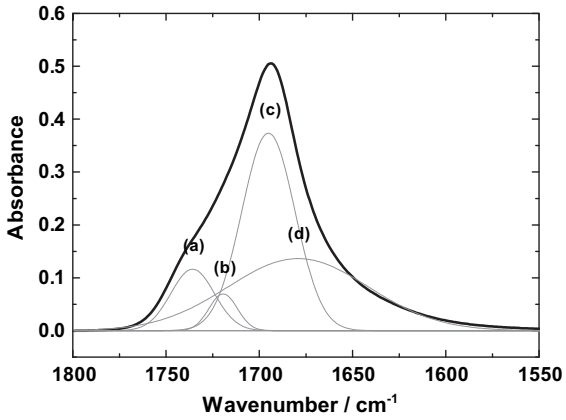

Fig. 3. An ATR-IR spectrum (heavy line) and its curve fitting spectra (thin line) of a dried PMAA film in the C═O stretching region. (a) monomer, (b) side-on dimer, (c) cyclic dimer and (d) linear oligomer structures of side-chain carboxyl groups in PMAA.

3.2. Time-resolved IR spectra

Fig. 4a and b represent time-resolved *in situ* ATR-IR spectra of a hydration process into a PMAA film collected every 0.20 s intervals and their second derivative spectra in the C═O stretching and finger print regions, respectively. An O–H deformation band of water at 1640 cm^{-1} increases with time, whereas other bands arising from PMAA decrease, due to swelling of the PMAA film by water sorption. Although the O–H deformation band is overlapped with the C═O stretching bands in the 1800–1600 cm^{-1} region, they are clearly distinguished by the second derivative spectra. The second derivative analysis shows that two of the four C═O stretching bands revealed by the curve fitting appear in the time-resolved spectra. A main peak at 1693 cm^{-1} and a higher wavenumber shoulder at 1740 cm^{-1} are assigned to cyclic dimers and free C═O groups of PMAA, respectively [29]. The main peak and the higher wavenumber shoulder shift by ca. 10 cm^{-1} to higher and lower wavenumber with time, respectively. In the finger print region, peaks located at 1262 and 1242 cm^{-1} assigned to the C–C–O stretching modes show a high wavenumber shift with time. The C–O–H bending and C–O stretching bands at 1185 and 1154 cm^{-1}, respectively, also shift during the water sorption progress. On the other hand, bands assigned to CH_2 and CH_3 groups shift slightly in the hydration process. These results imply that conformational changes due to hydration occur at around the carboxyl groups in PMAA.

The refractive index changed from 1.5 to 1.3 caused by the state changes from a solid film to hydrogel, and then there is a possibility that the absorbance of the peaks is affected. In this study, however, no C–H stretching and bending bands in the 3000–2900 cm^{-1} and 1500–1400 cm^{-1} regions, respectively, shifted in the time resolved spectra in Fig. 4b. Thus, there is little effect for band positions by the refractive index changes, and the structure changes of PMAA could be evaluated.

3.3. Quantum chemical calculations

Fig. 5A shows optimized structures and their simulated spectra of the (a) monomer, (b) cyclic dimer, (c) side-on dimer, (d) linear

Table 2
Observed frequencies of a C=O stretching band of PMAA and calculated frequencies of a C=O stretching band of PA, and hydrogen-bond energy calculated by QCCs. Indices of (a)–(h) correspond to the optimized structures shown in Fig. 5.

		Structures	Observed frequencies of C=O st. of PMAA [cm^{-1}]	Calculated frequencies of C=O st. of PA [cm^{-1}]	Calculated hydrogen-bond/hydration energy of PA [kcal/mol]
Hydrogen-bonded	a	Monomer	1736	1778	–
Structure	b	Cyclic dimer	1695	1722	19.5
	c	Side-on dimer	1719	1783, 1731	9.0
	d	Linear dimer	–	1755, 1741	9.1
	e	Linear trimer	–	1761, 1737, 1698	20.1
	–	Linear oligomer	1679	–	–
Hydration	f	Carbonyl hydrated	–	1748	7.1
Structure	g	Hydroxyl hydrated	–	1792	5.7
	h	Carboxylic acid hydrated	1708	1722	14.0

dimer and (e) linear trimer of PA. The observed vibrational frequencies of PMAA and the calculated ones of its model monomer, PA, in the C=O stretching region are summarized in Table 2. The calculated frequencies are obtained to compare with their observed and estimated C=O stretching bands. Compared with the calculated frequency of the free C=O stretching band of PA monomer (1778 cm^{-1}), the calculated frequencies of the hydrogen-bonds C=O stretching bands of the cyclic dimers, side-on dimers and linear oligomers of PA shift, respectively. With the increase in the PA molecules forming linear oligomers, the calculated frequency of the C=O stretching band shifts to a lower wavenumber and broadens. And the simulation supports that a overlapped linear oligomers band is broaden. These calculation results are in good agreement with the observed spectrum of the dried PMAA film shown in Figs. 2a and 3.

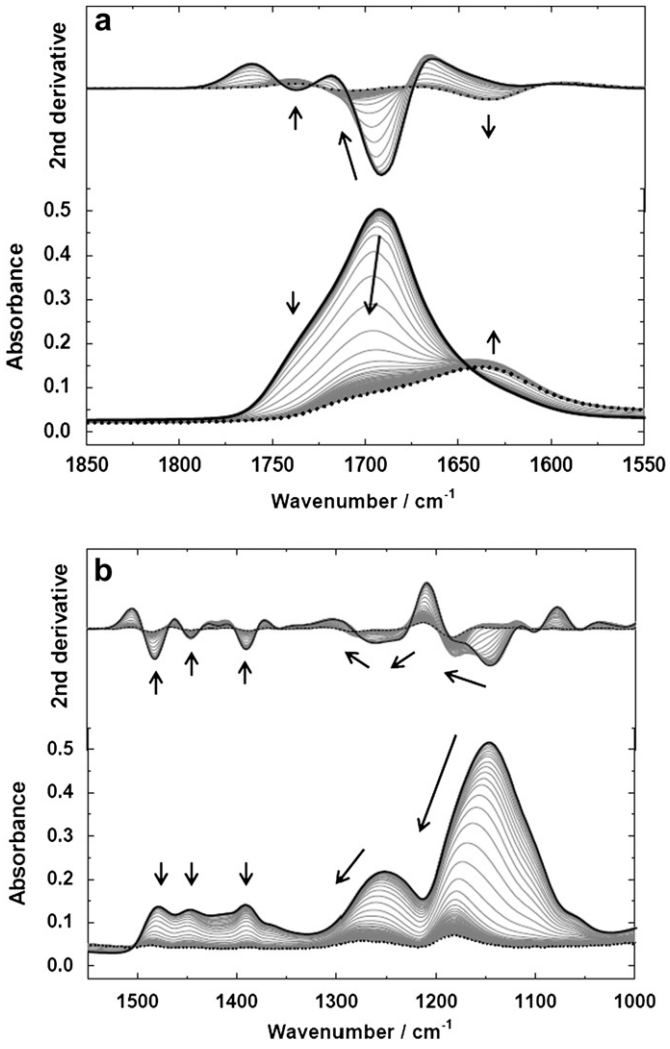

Fig. 4. Time-resolved ATR-IR spectra of the hydration process into a PMAA film by water (bottom) and their second derivative spectra (top) every 0.2 s between 0 and 30 s, (a) the C=O stretching and water O–H deformation region, and (b) finger print region, respectively. Before (heavy line) and after hydration (broken line).

Fig. 5B illustrates optimized structures and their simulated spectra of PA hydrated with (f) the carbonyl group, (g) the hydroxyl group and (h) the carboxyl group like side-on from. These results are also in accord with the observed one shown in Fig. 2d. The observed and calculated vibrational frequencies of hydrated PMAA and its hydration model monomer, PA, in the C=O stretching region are also summarized in Table 2. When the carbonyl groups of PA are hydrated (Fig. 5B(f) and (h)), the C=O stretching band is shifted to a lower frequency. Moreover, it was shown by their SCF energies that the latter structure is more stable than the former. On the other hand, when the oxygen atoms in hydroxyl groups are hydrated (Fig. 5B(g)), the C=O stretching band is moved to a higher frequency. Furthermore, Table 2 lists the intermolecular interaction energies of the respective structures. The calculated intermolecular interaction energies indicate that the cyclic dimer of PA is more stable than any other hydrogen-bonded structures of PA per a unit. Thus, the carboxyl groups of dried PMAA film may also form easily the cyclic dimer structures as the most stable structure. However, if the hydrated structures are included, the most stable structure is (h), the PA hydrated with the carboxyl group. Thus, the carboxyl groups of dried PMAA film may also form easily the side-on hydrated structures as the most stable structure after water penetration.

QQC is really useful and a solid investigation tool. However, we have to consider mainly a couple of the other critical parameters for the present calculations to acquire better agreements. One is the difference between the monomer and the polymer, and the other is the effect of environmental conditions. The former is concerned with a steric barrier of the polymer chain, while the latter contains a hydrophobic interaction among hydrophobic groups and a dielectric constant in water environment.

3.4. Hydration mechanism into a PMAA film

Fig. 6 shows time-dependent variations in the peak intensities and positions of the C=O stretching bands near 1736 and 1695 cm^{-1} and the O–H deformation band at 1628 cm^{-1} in the time-resolved spectra shown in Fig. 4a. The discussion regarding the peak intensities and positions are made in the narrow region of 1750–1680 cm^{-1} to prevent the effect of penetration depth of evanescent wave. Fig. 6a plots the time-dependent peak intensity changes of bands at 1695 and 1628 cm^{-1} due to the C=O stretching

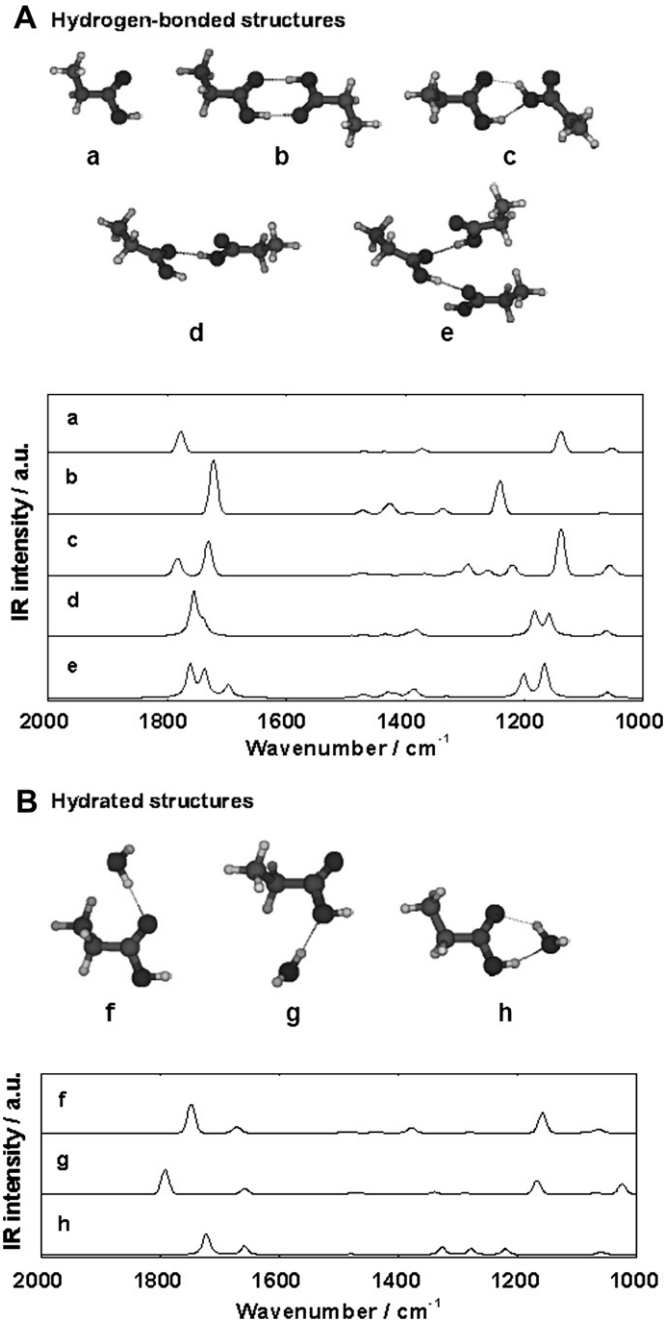

Fig. 5. Optimized structures and their simulated spectra obtained by QCCs. (A) Hydrogen-bonded structures; (a) PA monomer, (b) PA cyclic dimer, (c) PA side-on dimer, (d) PA linear dimer and (e) PA linear trimer. (B) Hydrated structures; (f) Hydrated with the carbonyl group, (g) Hydrated with the hydroxyl group and (h) Hydrated with the carboxyl group.

modes and the O–H deformation mode, respectively. These peak intensities begin to change at seven seconds after the water addition, and the intensity changes are almost completed in five seconds. Thus, the speed of the hydration process of the PMAA film is estimated to be ca. 0.18 $\mu m\, s^{-1}$. Furthermore, the gravimetric results demonstrate that 16 water molecules exist each methacrylic acid monomer unit in a swelled PMAA film. Consequently, there are a number of free water molecules which are not hydrated with the carboxyl groups in the hydrated PMAA film. Fig. 6b shows plots of time-dependent peak shifts of bands at 1736 and 1695 cm^{-1} due to the non-hydrogen-bonded and cyclic dimer C=O stretching

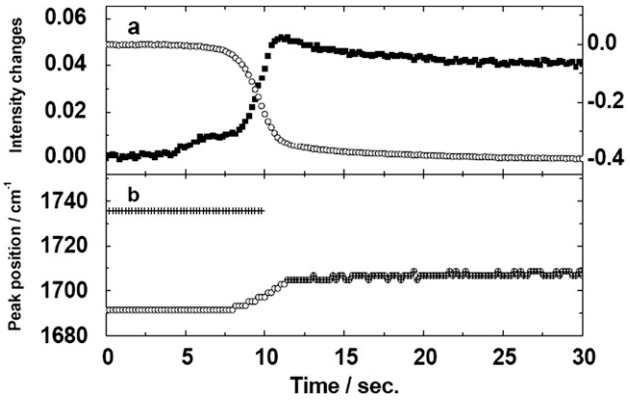

Fig. 6. (a) Time-dependent intensity changes in the O–H deformation band at 1628 cm^{-1} (■; on the left-hand scale) and the C=O stretching band at 1695 cm^{-1} of the cyclic dimer (o; on the right-hand scale) versus time. (b) Time-dependent peak shifts of the cyclic dimer C=O stretching band (o) and the non-hydrogen-bonded C=O stretching band at 1736 cm^{-1} (+) in the time-resolved spectra shown in Fig. 4.

modes, respectively. The peak position of cyclic dimer C=O stretching band at 1695 cm^{-1} shifts to a high frequency in parallel with the peak intensity attenuating. The free C=O stretching band at 1736 cm^{-1} also moves to a low frequency in parallel with the peak intensity decrease. Actually, there are some differences in frequencies of observed bands between the solid state and the hydrated samples due to the differences of physical characterization like permittivity and refractive index, however, the PMAA film was swelled and hydrated quickly after water penetration. Thus these bands could be assigned to each state, separately.

In the hydration process, the most stable cyclic dimer structure in the dried PMAA film is easily dissociated by the water storming and the hydrophobic interaction. Following that, the free carboxyl groups due to the dissociation of the cyclic dimers newly associate with water molecules to form more stable structure; hydrated structure with carboxylic groups in PMAA like side-on conformation. In other words, the hydration process of the carboxyl groups is induced by the dissociation of the hydrogen-bonded cyclic dimers in the dried state. They are supported by the above QCCs discussion. Thus, the other side-on and linear dimers, and oligomers which have weaker hydrogen-bond are also dissociated in the hydration process, and their non-hydrogen-bonded carboxylic groups newly associate with water molecules to form the same stable hydrated

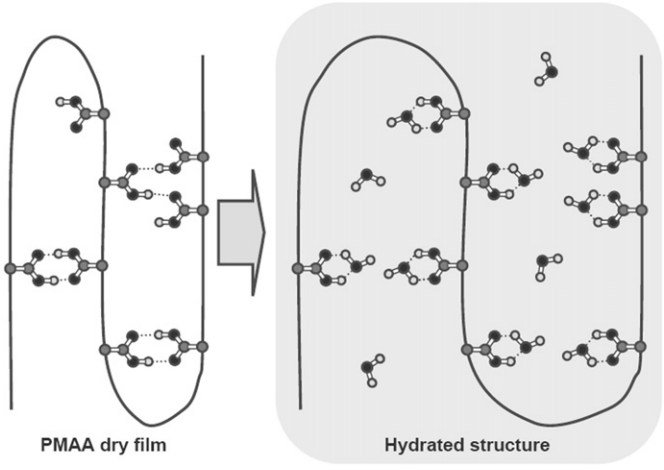

Fig. 7. The schematic illustration of the structure changes during hydration process of a PMAA film.

structure. Fig. 6 indicates that, the PMAA film is swelling by water absorption, and its carboxyl groups conformation changes from some kinds of hydrogen-bonded structures to entirely-different hydrated one occur in an instant.

4. Conclusions

A process of hydration into a PMAA film was investigated by time-resolved, *in situ*, ATR-IR spectroscopy. The present study has provided new insight into the hydration mechanism of carboxyl groups in the PMAA film. The intra- and inter-side-chain hydrogen-bonds in the PMAA are dissociated and the film is swelled by the water storming, then their generated non-hydrogen-bond carboxyl groups instantly hydrate with water molecules and equilibrate to the side-on form which is the most stable structure for the carboxyl groups (Fig. 7). The calculated frequencies and the interaction energies by QCCs using a model monomer of PA instead of PMAA have supported our spectral assignment and structure simulation of the hydrogen-bonded and the hydrated structures of PMAA.

Rapid-scan ATR-IR spectroscopy with a flow through cell is well suited to investigate hydration mechanisms of coating films using a stimulus-responsive polymer. Eventually, this sort of study may allow us to understand the dissolution mechanisms of pharmaceutical DDS products.

References

[1] Tahami KA, Singh J. Recent Pat Drug Deliv Formul 2007;1:65–71.
[2] Lin SY, Yu HL. J Polym Sci Part A Polym Chem 1999;37:2061–7.
[3] Victor SP, Sharma CP. J Biomater Appl 2002;17:125–34.
[4] The United States Pharmacopeia 31-National Formulary 26: The United States Pharmacopeial Convention; 2007. p. 267–274.
[5] European Pharmacopoeia, 6th ed.: European directorate for the quality of medicines; 2007. p. 266–275.
[6] Japanese Pharmacopoeia, 15th ed.: Society of Japanese pharmacopoeia; 2006. 116–120.
[7] Morita S, Tanaka M, Ozaki Y. Langmuir 2007;23:3750–61.
[8] Kitano H, Ichikawa K, Fukuda M, Mochizuki A, Tanaka M. J Colloid Interface Sci 2001;242:133–40.
[9] Kitano H, Ichikawa K, Ide M, Fukuda M, Mizuno W. Langmuir 2001;17:1889–95.
[10] Kusanagi H, Yukawa S. Polymer 1994;35:5637–40.
[11] Hajatdoost S, Yarwood J. J Chem Soc Faraday Trans 1997;93:1613–20.
[12] Pettersson A, Marino G, Pursiheimo A, Rosenholm JB. J Colloid Interface Sci 2000;228:73–81.
[13] Semmler J, Irish DE. J Solution Chem 1988;17:805–23.
[14] Genin F, Quiles F, Burneau A. Phys Chem Chem Phys 2001;3:932–42.
[15] Tanaka N, Kitano H, Ise N. J Phys Chem 1990;94:6290–2.
[16] Nishi N, Nakabayashi T, Kosugi K. J Phys Chem A 1999;103:10851–8.
[17] Nakabayashi T, Nishi N. J Phys Chem A 2002;106:3491–500.
[18] Flakus HT, Stachowska B. Chem Phys 2006;330:231–44.
[19] Flakus HT, Tyl A. Chem Phys 2007;336:36–50.
[20] Takahashi O, Yamanouchi S, Yamamoto K, Tabayashi K. Chem Phys Lett 2006;419:501–5.
[21] Asano A, Eguchi M, Kurotu T. J Polymer Science Part B Polymer Physics 1999;37:2007–12.
[22] Turi L, Dannenberg JJ. J Phys Chem 1933;97:12197–204.
[23] Brurneau A, Genin F, Quiles F. Phys Chem Chem Phys 2000;2:5020–9.
[24] Lourderaj U, Giri K, Sathyamurthy N. J Phys Chem A 2006;110:2709–17.
[25] Nakabayashi T, Kosugi K, Nishi N. J Phys Chem A 1999;103:8595–603.
[26] Zhang RQ, Wong NB, Lee ST, Zhu RS, Han KL. Chem Phys Lett 2000;319:213–9.
[27] Lewandosli H, Koglin E, Meier RJ. Vib Spectrosc 2005;39:15–22.
[28] Chuchev K, BelBruno JJ. J Mol Struc Theochem 2006;736:199–204.
[29] Dong J, Ozaki Y, Nakashima K. Macromolecules 1997;30:1111–7.
[30] Dong J, Tsubara N, Fujimoto Y, Ozaki Y, Nakashima K. Applied Spectrosc 2001;55:1603–9.
[31] Tanaka N, Kitano H, Ise N. J Phys Chem 1991;95:1503–7.
[32] Zhou Z, Shi Y, Zhou X. J Phys Chem A 2004;108:813–22.
[33] George L, Sander W. Spectrochim Acta Part A 2004;60:3225–32.
[34] Huang CF, Chang FC. Polymer 2003;44:2965–74.
[35] Chalmers JM, Griffiths PR. Handbook of vibrational spectroscopy; 2001.
[36] Savitzky A, Golay MJE. Anal Chem 1964;36:1627–39.
[37] Kawata S, Minami S. Appl Spectrosc 1984;38:49–58.
[38] Becke AD. J Chem Phys 1993;98:5648–52.
[39] Johnson BG, Frisch MJ. J Chem Phys 1994;100:7429–42.
[40] Frisch MJ, Trucks GW, Schlegel HB, Scuseria GE, Robb MA, Cheeseman JR, et al. Gaussian 03, revision B.05. Pittsburgh, PA: Gaussian, Inc.; 2003.
[41] Bauschlicher Jr CW, Partridge H. J Chem Phys 1995;103:1788–91.
[42] Onsager L. J Am Chem Soc 1938;58:1486.
[43] Wiberg KB, Murcko MA. J Phys Chem 1987;91:3616.